

Intervalley Polaron in Atomically Thin Transition Metal Dichalcogenides

M.M. Glazov, M.A. Semina
Ioffe Institute, 194021 St. Petersburg, Russia

C. Robert, B. Urbaszek, T. Amand, X. Marie
Université de Toulouse, INSA-CNRS-UPS, LPCNO, 135 Av. Rangueil, 31077 Toulouse, France

We study theoretically intervalley coupling in transition-metal dichalcogenide monolayers due to electron interaction with short-wavelength phonons. We demonstrate that this intervalley polaron coupling results in (i) a renormalization of the conduction band spin splitting and (ii) an increase of the electron effective masses. We also calculate the renormalization of the cyclotron energy and the Landau level splitting in the presence of an external magnetic field. An inter-valley magneto-phonon resonance is uncovered. Similar, but much weaker effects are also expected for the valence band holes. These results might help to resolve the discrepancy between *ab initio* values of the electron effective masses and the ones deduced from magneto-transport measurements.

Introduction. Fascinating electronic and optical properties of two-dimensional (2D) materials like graphene, transition-metal dichalcogenide (TMD) monolayers (MLs), atomically-thin hexagonal boron nitride, black phosphorus, and others have attracted strong interest [1–3]. Unusual band structure of TMD MLs with two valleys in conduction and valence bands, where the spin degeneracy of the electron and hole states is removed and the spin and valley degrees of freedom are locked [4, 5] has made 2D TMD crystals extremely attractive for study of spintronic and valleytronic effects [6–9]. Chiral selection rules combined with strong excitonic effects provide unprecedented access to spin and valley indices of charge carriers by optical means [10, 11]. For in-depth studies of TMD MLs and the development of possible applications, the basic band structure parameters, including band gap and effective masses should be reliably established both from experiments and modeling.

Optical spectroscopy has made it possible to determine key parameters such as exciton band gap, binding energy, Landé factor and evaluate the reduced masses of the electron-hole pairs from the high-magnetic field experiments [10, 12]. The single electron parameters, namely, the effective masses of charge carriers and their individual g factors are usually hard to determine optically. These quantities are, as a rule, inferred from transport measurements. Thanks to the improvement of carrier mobility obtained in hBN encapsulated TMD monolayers [13, 14], quantum transport measurements have been recently performed.

Observation of Landau levels has allowed one to determine the effective masses of the charge carriers in the valence and conduction band [14–18]. Interestingly, while the measured valence band hole (VB) masses are in good agreement with both first-principles modeling and angle resolved photoemission spectroscopy (ARPES) measurements [19, 20], the discrepancies for the conduction band (CB) effective masses in Mo-based monolayers are substantial [16, 17] and can hardly be related to electron-electron interaction and inaccuracies in density functional theory (DFT) calculations. The trans-

port measurements in both MoS₂ and MoSe₂ MLs yield characteristic CB electron effective mass of 0.7–0.8 m_0 , typically twice larger than the ones deduced from DFT calculations (m_0 is the free electron mass) [21, 22].

Here we demonstrate a pathway which could improve the agreement between the theory and the experiment for conduction band masses in TMD MLs. We show that two valleys \mathbf{K} and \mathbf{K}' can be coupled by the phonons with wavevectors close to the edge of the Brillouin zone (BZ). Let us recall that the spin up and the spin down CB bands in each non-equivalent valley \mathbf{K} and \mathbf{K}' are split by the spin-orbit (SO) interaction, with a typical energy difference, Δ_{cb} , of a few tens of meV, see Fig. 1 [21, 23]. The intervalley electron-phonon coupling is stronger for the CB because electron-phonon interaction is largely spin-conserving, thus strong SO splitting of VB (of the order of hundreds of meV) suppresses the mixing. We develop an analytical model for this new type of polaron and demonstrate that the intervalley polaron effect results in the renormalization of both the CB spin splitting and the effective masses of the electrons. We discuss also the renormalization of the Landau level energies due to the intervalley electron-phonon interaction. Our simple model indicates an increase of the electron effective mass due to inter-valley polaron, in qualitative agreement with transport measurements, but the quantitative agreement with the experiments requires exaggerated coupling constant possibly due to oversimplification of the model.

Intervalley electron-phonon interaction. Electrons propagating through the crystal interact with the host lattice atoms and produce local deformations of the lattice. Thus, the periodic potential experienced by the electron is modified resulting in a modification of the electron energy, and the dragging of the crystal lattice deformation with the electron gives rise to an increase of electrons effective mass as a result of the polaron effect [24–28]. This effect was found to be important to explain effective mass variations in many different semiconductors [29–32]. Quantum mechanically, electron-phonon interaction due to virtual processes of emission and reabsorption of the phonon by the electron gives rise to the formation of the

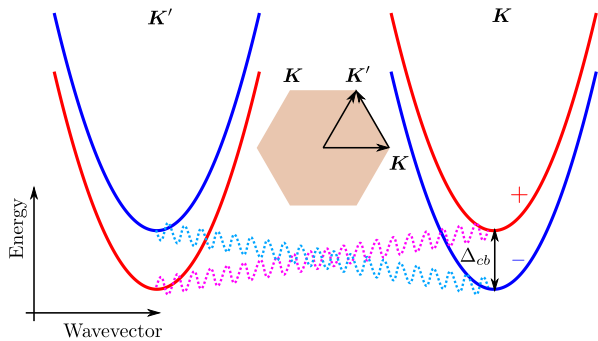


Figure 1. Schematic illustration of the conduction subbands in the vicinity of the \mathbf{K} and \mathbf{K}' points at the BZ edge. Inset shows hexagonal BZ. Wiggly lines illustrate phonon-induced coupling between the valleys. Signs “+” and “-” denote top and bottom subbands.

phonon cloud surrounding the electron and renormalizes its dispersion. In the second-order perturbation theory the electron self-energy, $\Sigma_{\mathbf{p}}(\varepsilon)$, due to the coupling with phonons can be written at zero temperature as

$$\Sigma_{\mathbf{p}}(\varepsilon) = \sum_{\mathbf{q}, \alpha; j} \frac{|M_{\mathbf{q}, \alpha}^j|^2}{\varepsilon - \hbar\Omega_{\mathbf{q}, \alpha} - E_{\mathbf{p}-\mathbf{q}}^j + i\delta}. \quad (1)$$

Here \mathbf{p} is the electron wavevector in the crystal, ε is the energy variable, \mathbf{q} is the phonon wavevector, α enumerates the phonon branches, j enumerates the intermediate states of the electron, $M_{\mathbf{q}, \alpha}^j$ is the electron-phonon coupling matrix element, $\Omega_{\mathbf{q}, \alpha}$ is the frequency of the corresponding phonon mode and $E_{\mathbf{p}}^j$ is the electron dispersion in the state j , the term with $\delta \rightarrow +0$ in the denominator ensures the causality. The self-energy (1) describes the electron energy and dispersion renormalization in the second order in the electron phonon interaction.

Leading contributions to Eq. (1) are provided mainly by nearest intermediate states and also by high-symmetry points of the BZ where the phonon dispersion is flat and the density of states is increased [33]. Analysis of the TMD MLs CB structure shows that the main contributions to the self-energy are produced by the intermediate states in the same band and the same valley, i.e., by the standard, *intravalley*, Fröhlich-like polaron, studied, e.g., in Refs. [34–36] as well as by the intermediate states in the opposite valley (\mathbf{K}' for the electrons in the \mathbf{K} valley and vice versa), which result in the *intervalley* polaron, not investigated so far. Key difference for the intervalley polaron compared with the intravalley polaron is the presence of the CB spin splitting in the energy denominator.

The results on intravalley polaron are summarized in the supplementary information (SI), which also contains justification of applicability of the second-order perturbation theory to calculate $\Sigma_{\mathbf{p}}(\varepsilon)$ in Eq. (1) for the TMD ML system [37]. Here we focus on the new intervalley polaron which results in the coupling of electron states in \mathbf{K} and \mathbf{K}' valleys as schematically shown in Fig. 1. Generally, in order to calculate the self energy, the electron

and phonon dispersions across the whole BZ are needed; here we take into account the contribution coming from the vicinity of \mathbf{K}' (for \mathbf{K} valley electron) where the density of states is largest. We focus on the renormalization of electron states in the \mathbf{K} valley, correspondingly, we replace $M_{\mathbf{q}, \alpha}^i$ by $M_{\mathbf{K}, \alpha}^i$, its value for $\mathbf{q} = \mathbf{K}$, we also disregard the phonon dispersion replacing $\hbar\Omega_{\mathbf{q}, \alpha}$ by $\hbar\Omega_{\mathbf{K}, \alpha}$. In what follows we omit the subscript α (keeping in mind that in the final result one has to sum over all appropriate phonon modes) and take into account that the spin is conserved by the electron-phonon interaction. Changing the integration variable from \mathbf{q} to $\mathbf{q}' = \mathbf{q} - \mathbf{K}$, and taking into account that for the electron in the top (bottom) spin subband the intermediate state energy reads $E_{\mathbf{p}-\mathbf{q}}^j \approx \mp\Delta_{cb} + E_{\mathbf{p}-\mathbf{q}'}$, $E_{\mathbf{p}} = \hbar^2 p^2 / (2m)$, where m being the bare CB effective mass [50], we arrive at

$$\Sigma_{\mathbf{p}, \pm}(\varepsilon) = -\frac{\beta_{\mathbf{K}}(\Delta_{cb} + \hbar\Omega_{\mathbf{K}})}{4\pi} \times \int_0^{E_Q} \frac{dE}{\sqrt{(\varepsilon - E_{\mathbf{p}} \pm \Delta_{cb} - \hbar\Omega_{\mathbf{K}} - E)^2 - 4E_{\mathbf{p}}E}}. \quad (2)$$

Here subscripts correspond to the top (+) and bottom (-) spin subbands, $\Delta_{cb} > 0$. An effective dimensionless intervalley coupling constant in Eq. (2) reads

$$\beta_{\mathbf{K}} = \frac{2\mathcal{S}m|M_{\mathbf{K}}|^2}{\hbar^2(\Delta_{cb} + \hbar\Omega_{\mathbf{K}})}, \quad (3)$$

and the cut-off energy $E_Q = \hbar^2 Q^2 / 2m$ with the cut-off wavevector $Q \sim |\mathbf{K}|$ is needed to avoid the logarithmic divergence of the integral, \mathcal{S} is the normalization area. We have omitted infinitesimal term $i\delta$ in the denominator for brevity. It is worth stressing that $\beta_{\mathbf{K}}$ depends not only on the matrix element of the electron-phonon intervalley interaction but also on the combination of the CB spin splitting and the phonon energy $\Delta_{cb} + \hbar\Omega_{\mathbf{K}}$. The logarithmic divergence does not mean particularly strong electron-phonon coupling, it demonstrates the limitations of analytical approach with parabolic bands, flat dispersion of phonons and momentum-independent coupling.

Renormalization of band parameters. The electron-phonon interaction produces noticeable effect on conduction subband energies [51]. We predict a significant renormalization effect of the CB spin splitting. Indeed, as it is seen from Fig. 1, for the electron in the lower spin subband the intermediate state has a higher energy, $\Delta_{cb} + \hbar\Omega_{\mathbf{K}}$, while for the electron in the higher spin subband the intermediate state has a lower energy, $-\Delta_{cb} + \hbar\Omega_{\mathbf{K}}$. Under the condition $\hbar\Omega_{\mathbf{K}} > \Delta_{cb}$ both subbands are pushed by the electron-phonon interaction towards the lower energies, but the shift of the upper subband is larger, see inset in Fig. 2. The variation of the CB spin splitting can be recast as

$$\delta\Delta_{cb} = \lim_{p \rightarrow 0} [\Sigma_{\mathbf{p}, +}(E_{\mathbf{p}}) - \Sigma_{\mathbf{p}, -}(E_{\mathbf{p}})]. \quad (4)$$

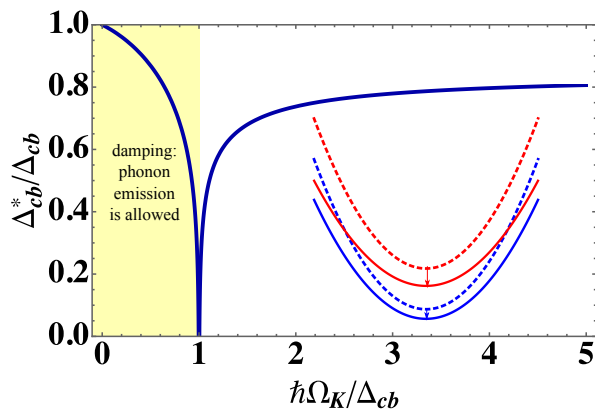


Figure 2. Renormalized conduction band spin splitting as a function of the ratio between the phonon energy $\hbar\Omega_{\mathbf{K}}$ and bare conduction band spin splitting Δ_{cb} calculated for $\beta_{\mathbf{K}} = 1$ after Eq. (5). Filled area corresponds to the situation where $\hbar\Omega_{\mathbf{K}} < \Delta_{cb}$ and the real phonon emission processes are possible. Inset demonstrates relative shifts of upper and lower spin subbands in one valley due to the electron-phonon interaction with another valley and the renormalization of the effective mass (exaggerated for illustration).

We introduce the renormalized CB spin splitting $\Delta_{cb}^* = \Delta_{cb} + \text{Re}\{\delta\Delta_{cb}\}$ and present it in the form

$$\Delta_{cb}^* = \Delta_{cb} \left[1 - \frac{\beta_{\mathbf{K}}}{4\pi} \left(1 + \frac{\hbar\Omega_{\mathbf{K}}}{\Delta_{cb}} \right) \ln \left(\frac{\hbar\Omega_{\mathbf{K}} + \Delta_{cb}}{\hbar\Omega_{\mathbf{K}} - \Delta_{cb}} \right) \right]. \quad (5)$$

Note that logarithmic divergencies in the self-energies cancel and the result (5) does not depend on the cut-off energy. For $\Delta_{cb} > \hbar\Omega_{\mathbf{K}}$ the argument of the logarithm becomes negative and, formally, Δ_{cb}^* acquires an imaginary part. In this case, the energy shift is given by the real part of the same expression (5). However, the intervalley transitions from the upper to the lower subband accompanied by the phonon emission become possible. The associated damping of the electron in the upper spin subband is determined by the imaginary part of Δ_{cb}^* . The calculated renormalization of the CB spin splitting is plotted in Fig. 2 as a function of the ratio $\hbar\Omega_{\mathbf{K}}/\Delta_{cb}$. The singularity in the Δ_{cb}^* at $\hbar\Omega_{\mathbf{K}} = \Delta_{cb}$, i.e., at the threshold of the phonon emission, results from the resonance condition where the energy of the electron in the top subband minus phonon energy equals the energy of the electron in the bottom subband. The detailed analysis of this singular behavior can be carried out by the methods developed in Ref. [52]; it is beyond the scope of the present work.

Similarly, one can extract the p^2 contribution in the self-energy and obtain the renormalization of the effective mass resulting from the intervalley polaron. We obtain for the top (+) and bottom (-) spin subbands

$$m_{\pm}^* = m \left(1 + \frac{\beta_{\mathbf{K}}}{4\pi} \frac{\hbar\Omega_{\mathbf{K}} + \Delta_{cb}}{\hbar\Omega_{\mathbf{K}} \mp \Delta_{cb}} \right). \quad (6)$$

Interestingly, the polaron effect does not only increase

the effective masses but also leads to a difference of the mass of the two spin subbands: $m_+^* \neq m_-^*$. Similarly to the renormalization of the Δ_{cb} the intervalley polaron effect on the masses is singular at $\hbar\Omega_{\mathbf{K}} = \Delta_{cb}$, i.e., at the threshold of the phonon emission. Interestingly, the intervalley polaron effect makes both spin subbands heavier and the renormalization of the mass in the topmost subband is larger, $m_+^* > m_-^*$ (inset in Fig. 2). Note that the interaction of the CBs with the VBs ($\mathbf{k} \cdot \mathbf{p}$ mixing) also yields a slight difference of masses for top and bottom CBs; this difference is controlled by the dimensionless $\sim \Delta_{vb}/E_g$ where E_g is the band gap and Δ_{vb} the SO splitting of the VB [11, 21]. In contrast to the intervalley polaron effect, this $\mathbf{k} \cdot \mathbf{p}$ -mixing of the bands together with the SO coupling makes topmost subband heavier in Mo-based MLs and lighter in W-based MLs due to different order of spin states [21].

Renormalization of Landau levels. Let us now discuss the effect of the intervalley polaron on the electron spectrum in magnetic field. We assume that the magnetic field is applied perpendicular to the ML plane and disregard the electron Zeeman splitting assuming it to be much smaller than both the phonon energy $\hbar\Omega_{\mathbf{K}}$ and the CB SO splitting Δ_{cb} . As a result, in the absence of electron-phonon interaction, the electron energy spectrum consists of the well-known series of Landau levels

$$E_n = \hbar\omega_c \left(n + \frac{1}{2} \right), \quad (7)$$

where $\omega_c = |eB_z/mc|$ is the electron cyclotron frequency. We calculate the correction to the energy of n -th Landau level in the second order in the intervalley electron-phonon interaction. Similarly to Eqs. (1) and (2) we obtain (cf. Ref. [35] where intravalley Fröhlich magnetopolaron in TMD ML was studied)

$$\delta E_{n,\pm} = \sum_{\mathbf{q}', n', k'_y} \frac{|M_{\mathbf{K}}|^2 \left| \langle n' k'_y | e^{i\mathbf{q}'\cdot\mathbf{r}} | n k_y \rangle \right|^2}{\hbar\omega_c(n - n') - \hbar\Omega_{\mathbf{K}} \pm \Delta_{cb}}. \quad (8)$$

Here we disregarded the wavevector dependence of the intervalley matrix element and phonon dispersion, \pm refers to the electron in the top and bottom spin subbands, $\mathbf{q}' = \mathbf{q} - \mathbf{K}$ with \mathbf{q} is the phonon wavevector, $|n k_y\rangle$ is the electron state in the Landau gauge, n is the Landau level number, k_y is the component of the electron inplane wavevector. We obtain the renormalized electron spectrum in the form of Eq. (8) with the effective cyclotron frequency $\omega_{c,\pm}^*(n)$ which depends now on the Landau level number and on the spin subband [37]:

$$\frac{\omega_{c,\pm}^*(n)}{\omega_c} = 1 - \frac{\beta_{\mathbf{K}}}{4\pi(1 - \eta_{\pm}n)} \frac{\hbar\Omega_{\mathbf{K}} + \Delta_{cb}}{\hbar\Omega_{\mathbf{K}} \mp \Delta_{cb}}, \quad (9)$$

where $\eta_{\pm} = \hbar\omega_c/(\hbar\Omega_{\mathbf{K}} \mp \Delta_{cb})$ characterizes the magnetic field strength.

In the limit of weak magnetic fields and low Landau levels, where $\eta_{\pm}n \ll 1$, we have series of equidistant Lan-

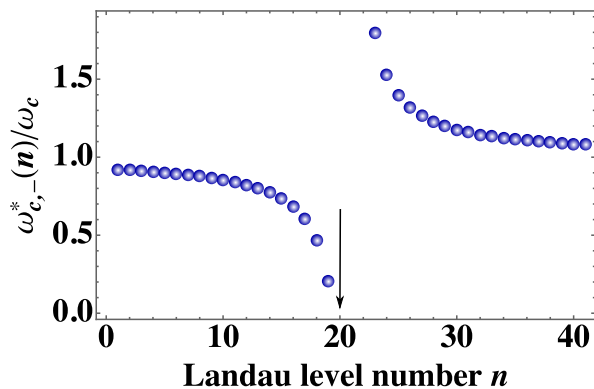


Figure 3. Renormalized cyclotron frequency for the bottom spin subband at $\beta_{\mathbf{K}} = 1$ and $\hbar\omega_c/(\hbar\Omega_{\mathbf{K}} + \Delta_{cb}) = 1/20$ calculated after Eq. (9). The arrow indicates intervalley magneto-phonon resonance condition, Eq. (10).

dau levels in each subband with the renormalized effective mass given by Eq. (6). For $\eta_{\pm}n \gg 1$ one recovers unperturbed Landau Levels, Eq. (8), because phonon cloud cannot follow the electron orbiting with high enough frequency. Strong renormalization of the cyclotron frequency occurs for the top spin subband at $\hbar\Omega_{\mathbf{K}} = \Delta_{cb}$ where resonant emission of phonons becomes possible. Another strong feature in $\omega_{c,\pm}^*(n)$ occurs at

$$n = \left\lfloor \frac{1}{\eta_{\pm}} \right\rfloor, \quad (10)$$

where $\lfloor \dots \rfloor$ stands for the integer part. Under this condition there is an intervalley magneto-phonon resonance (cf. Refs. [53, 54]): The energy of n -th Landau level in one of the subbands is at resonance with the bottom of another subband in the opposite valley. In this case the polaron effect is particularly strong.

Discussion. Intervalley polaron coupling in TMD MLs can be enabled by the phonons with large wavevectors $|\mathbf{q}| \approx |\mathbf{K}|$ [6, 55–57]. The symmetry of relevant phonon modes is discussed in SI, for conduction band the main contribution comes from the chiral phonon mode [6, 58, 59] whose angular momentum component equals to ± 1 for $\mathbf{K}' \rightleftharpoons \mathbf{K}$ transfer [37]. The effect is related to the intervalley deformation potential induced by the lattice vibrations. Note that the Fröhlich interaction is long-range and expected to provide negligible contribution to the intervalley polaron effect. The matrix element $M_{\mathbf{K}}$ in Eqs. (3) and (8) can be represented as

$$M_{\mathbf{K}} = \sqrt{\frac{\hbar}{2\rho\Omega_{\mathbf{K}}\mathcal{S}}} D_0, \quad (11)$$

where ρ is the two-dimensional mass density of the crystal and D_0 is the deformation potential parameter, \mathcal{S} is the normalization area. Substituting Eq. (11) into Eq. (3) we obtain a crude estimate for the coupling strength $\beta_{\mathbf{K}}$:

$$\beta_{\mathbf{K}} \sim \frac{D_0^2}{\hbar\Omega_{\mathbf{K}}(\hbar\Omega_{\mathbf{K}} + \Delta_{cb})} \frac{m}{\rho} \sim 0.1 \dots 1, \quad (12)$$

at $\rho = 3 \times 10^{-7}$ g/cm², $m = 0.5m_0$, $D_0 \sim (1 \dots 4) \times 10^8$ eV/cm [57] and $\hbar\Omega_{\mathbf{K}} \sim \Delta_{cb} \sim 10$ meV. With this simplified model and the uncertainty of the parameters involved, we find that the coupling is not particularly strong. It will yield an increase of the bottom CB mass by $\sim 10\%$. We emphasize that the exact values of key parameters such as the CB SO splitting and deformation potential parameters are not very well known. The CB SO splitting strongly varies for different DFT models [60]. The deformation potential can be roughly estimated as the ratio of atomic energy scale, ~ 10 eV, to the lattice constant (several Angstrom) resulting in values consistent with Ref. [57]. Additional enhancement is expected for the CB states due to the presence of the \mathbf{Q} (also denoted as $\mathbf{\Lambda}$) valley. The coupling constant $\beta_{\mathbf{Q}}$ of the intervalley polaron involving the \mathbf{Q} -valley has a similar order of magnitude.

This increase of the CB electron mass in TMD monolayer could qualitatively explain the recent measurements performed on high-quality n -type MoS₂ and MoSe₂ monolayers displaying well resolved Shubnikov de Haas oscillations. These experiments yield CB mass of about $0.7m_0$ in MoS₂ MLs and $0.8m_0$ in MoSe₂ ML [16, 17]. Surprisingly the masses calculated with DFT approaches are much smaller, typically $(0.4 - 0.5)m_0$ for both MLs [21, 22]. This can hardly be explained by the electron-electron interaction as the measured electron mass for both systems does not depend much on the doping density. Remarkably this discrepancy between experiment and DFT calculation does not occur for the VB, where both transport [15] and ARPES [19, 20] measurements yield the effective mass of about $0.4m_0$, in agreement with the DFT calculations [61]. The standard Fröhlich polaron effect could not explain the increase of mass observed for CB only as it should affect in a similar manner both electrons and holes. The same argument rules out possible effects of interfacial polarons due to electron-phonon coupling at the interfaces between the TMD ML and hBN [62]. In contrast, the intervalley polaron effect, as explained above, yields an increase of the CB mass (compared to the mass calculated with DFT) but produces negligible effect on the VB mass because of much larger VB SO splitting. Estimates after Eq. (12) for the VB yields the value $\beta_{\mathbf{K}}^{vb} \sim (\hbar\Omega_{\mathbf{K}} + \Delta_{cb})/\Delta_{vb}\beta_{\mathbf{K}} \sim \beta_{\mathbf{K}}/10$. Recent magneto-optical spectroscopy of TMD MLs [63] reveals an increase in m in Mo-based MLs, indicating the importance of the intervalley polaron effect for magnetoexcitons

Our calculations also predict a significant decrease of the CB SO splitting due to intervalley polaron effect (Fig. 2). We suggest that the polaron effect should be taken into account when comparing measured SO [16, 17] values to DFT.

The intervalley polaron mixes bright and momentum-forbidden excitonic states and does not affect the optical selection rules in no-phonon transitions, but polaron formation could influence the spin and valley relaxation.

Conclusion. We have developed the theory of a

novel type of polaron corresponding to phonon-induced coupling between the two non equivalent valleys of transition-metal dichalcogenide monolayers. This intervalley polaron associated to short-wavelength phonons results in both an increase of the electron effective mass and a decrease of the conduction band spin-orbit splitting. In the presence of an external magnetic field it will also lead to the renormalization of the cyclotron energy and the Landau level splitting. In contrast the intervalley polaron has negligible effects on the valence band due

to its much larger spin-orbit splitting.

Acknowledgements. We are grateful to H. Dery for very stimulating discussions. M.A.S. and M.M.G. acknowledge partial support from LIA ILNACS through the RFBR project 17-52-16020. M.M.G. was partially supported by the RFBR project 17-02-00383. M.A.S. also acknowledges partial support of the Government of the Russian Federation (Project No. 14.W03.31.0011 at the Ioffe Institute). We acknowledge funding from ANR 2D-vdW-Spin, ANR VallEx and ANR MagicValley. X.M. also acknowledges the Institut Universitaire de France.

-
- [1] A. K. Geim and K. S. Novoselov, The rise of graphene, *Nat Mater* **6**, 183 (2007).
- [2] A. K. Geim and I. V. Grigorieva, Van der Waals heterostructures, *Nature* **499**, 419 (2013).
- [3] P. Ajayan, P. Kim, and K. Banerjee, van der Waals materials, *Physics Today* **69**, 9 (2016).
- [4] D. Xiao, G.-B. Liu, W. Feng, X. Xu, and W. Yao, Coupled spin and valley physics in monolayers of MoS₂ and other group-VI dichalcogenides, *Phys. Rev. Lett.* **108**, 196802 (2012).
- [5] X. Xu, W. Yao, D. Xiao, and T. F. Heinz, Spin and pseudospins in layered transition metal dichalcogenides, *Nat Phys* **10**, 343 (2014).
- [6] Y. Song and H. Dery, Transport theory of monolayer transition-metal dichalcogenides through symmetry, *Phys. Rev. Lett.* **111**, 026601 (2013).
- [7] H. Dery and Y. Song, Polarization analysis of excitons in monolayer and bilayer transition-metal dichalcogenides, *Physical Review B* **92**, 125431 (2015).
- [8] G. Wang, C. Robert, M. M. Glazov, F. Cadiz, E. Courtade, T. Amand, D. Lagarde, T. Taniguchi, K. Watanabe, B. Urbaszek, and X. Marie, In-plane propagation of light in transition metal dichalcogenide monolayers: Optical selection rules, *Phys. Rev. Lett.* **119**, 047401 (2017).
- [9] P. Dey, L. Yang, C. Robert, G. Wang, B. Urbaszek, X. Marie, and S. A. Crooker, Gate-controlled spin-valley locking of resident carriers in WSe₂ monolayers, *Phys. Rev. Lett.* **119**, 137401 (2017).
- [10] G. Wang, A. Chernikov, M. M. Glazov, T. F. Heinz, X. Marie, T. Amand, and B. Urbaszek, Colloquium: Excitons in atomically thin transition metal dichalcogenides, *Rev. Mod. Phys.* **90**, 021001 (2018).
- [11] M. V. Durnev and M. M. Glazov, Excitons and trions in two-dimensional semiconductors based on transition metal dichalcogenides, *Physics-Uspekhi* **61**, 825 (2018).
- [12] A. V. Stier, N. P. Wilson, K. A. Velizhanin, J. Kono, X. Xu, and S. A. Crooker, Magneto-optics of exciton rydberg states in a monolayer semiconductor, *Phys. Rev. Lett.* **120**, 057405 (2018).
- [13] F. Cadiz, E. Courtade, C. Robert, G. Wang, Y. Shen, H. Cai, T. Taniguchi, K. Watanabe, H. Carrere, D. Lagarde, *et al.*, Excitonic linewidth approaching the homogeneous limit in MoS₂-based van der waals heterostructures, *Phys. Rev. X* **7**, 021026 (2017).
- [14] M. V. Gustafsson, M. Yankowitz, C. Forsythe, D. Rhodes, K. Watanabe, T. Taniguchi, J. Hone, X. Zhu, and C. R. Dean, Ambipolar Landau levels and strong band-selective carrier interactions in monolayer WSe₂, *Nature Materials* **17**, 411 (2018).
- [15] B. Fallahazad, H. C. P. Movva, K. Kim, S. Larentis, T. Taniguchi, K. Watanabe, S. K. Banerjee, and E. Tutuc, Shubnikov-de Haas oscillations of high-mobility holes in monolayer and bilayer WSe₂: Landau level degeneracy, effective mass, and negative compressibility, *Phys. Rev. Lett.* **116**, 086601 (2016).
- [16] S. Larentis, H. C. P. Movva, B. Fallahazad, K. Kim, A. Behroozi, T. Taniguchi, K. Watanabe, S. K. Banerjee, and E. Tutuc, Large effective mass and interaction-enhanced Zeeman splitting of *K*-valley electrons in MoSe₂, *Phys. Rev. B* **97**, 201407 (2018).
- [17] R. Pisoni, A. Kormányos, M. Brooks, Z. Lei, P. Back, M. Eich, H. Overweg, Y. Lee, P. Rickhaus, K. Watanabe, T. Taniguchi, A. Imamoglu, G. Burkard, T. Ihn, and K. Ensslin, Interactions and magnetotransport through spin-valley coupled Landau levels in monolayer MoS₂, *Phys. Rev. Lett.* **121**, 247701 (2018).
- [18] J. Lin, T. Han, B. A. Piot, Z. Wu, S. Xu, G. Long, L. An, P. Cheung, P.-P. Zheng, P. Plochocka, X. Dai, D. K. Maude, F. Zhang, and N. Wang, Determining interaction enhanced valley susceptibility in spin-valley-locked MoS₂, *Nano Letters* **10.1021/acs.nanolett.8b04731** (2019).
- [19] Y. Zhang, T.-R. Chang, B. Zhou, Y.-T. Cui, H. Yan, Z. Liu, F. Schmitt, J. Lee, R. Moore, Y. Chen, H. Lin, H.-T. Jeng, S.-K. Mo, Z. Hussain, A. Bansil, and Z.-X. Shen, Direct observation of the transition from indirect to direct bandgap in atomically thin epitaxial MoSe₂, *Nature Nanotechnology* **9**, 111 (2013).
- [20] W. Jin, P.-C. Yeh, N. Zaki, D. Zhang, J. T. Sadowski, A. Al-Mahboob, A. M. van Der Zande, D. A. Chenet, J. I. Dadap, I. P. Herman, *et al.*, Direct measurement of the thickness-dependent electronic band structure of MoS₂ using angle-resolved photoemission spectroscopy, *Phys. Rev. Lett.* **111**, 106801 (2013).
- [21] A. Kormanyos, G. Burkard, M. Gmitra, J. Fabian, V. Zolyomi, N. D. Drummond, and V. Fal'ko, *k · p* theory for two-dimensional transition metal dichalcogenide semiconductors, *2D Materials* **2**, 022001 (2015).
- [22] D. Wickramaratne, F. Zahid, and R. K. Lake, Electronic and thermoelectric properties of few-layer transition metal dichalcogenides, *The Journal of chemical physics* **140**, 124710 (2014).
- [23] K. Kośmider, J. W. González, and J. Fernández-Rossier, Large spin splitting in the conduction band of transi-

- tion metal dichalcogenide monolayers, *Phys. Rev. B* **88**, 245436 (2013).
- [24] L. D. Landau, Über die bewegung der elektronen in kristallgitter, *Phys. Z. Sowjetunion.* **3**, 644 (1933).
- [25] S. I. Pekar, Local quantum states of electrons in an ideal ion crystal, *Zh. Eksp. Teor. Fiz* **16**, 341 (1946).
- [26] L. D. Landau and S. I. Pekar, Effective mass of a polaron, *Zh. Eksp. Teor. Fiz.* **18**, 419 (1948).
- [27] H. Fröhlich, Electrons in lattice fields, *Advances in Physics* **3**, 325 (1954).
- [28] A. S. Alexandrov and J. T. Devreese, *Advances in Polaron Physics* (Springer Berlin Heidelberg, 2010).
- [29] M. Grynberg, S. Huant, G. Martinez, J. Kossut, T. Wojtowicz, G. Karczewski, J. M. Shi, F. M. Peeters, and J. T. Devreese, Magnetopolaron effect on shallow indium donors in cdte, *Phys. Rev. B* **54**, 1467 (1996).
- [30] G. Ploner, J. Smoliner, G. Strasser, M. Hauser, and E. Gornik, Energy levels of quantum wires determined from magnetophonon resonance experiments, *Phys. Rev. B* **57**, 3966 (1998).
- [31] T. Itoh, M. Nishijima, A. I. Ekimov, C. Gourdon, A. L. Efros, and M. Rosen, Polaron and exciton-phonon complexes in CuCl nanocrystals, *Phys. Rev. Lett.* **74**, 1645 (1995).
- [32] J. L. M. van Mechelen, D. van der Marel, C. Grimaldi, A. B. Kuzmenko, N. P. Armitage, N. Reyren, H. Hagemann, and I. I. Mazin, Electron-phonon interaction and charge carrier mass enhancement in SrTiO₃, *Phys. Rev. Lett.* **100**, 226403 (2008).
- [33] D. Christiansen, M. Selig, G. Berghäuser, R. Schmidt, I. Niehues, R. Schneider, A. Arora, S. M. de Vasconcelos, R. Bratschitsch, E. Malic, *et al.*, Phonon sidebands in monolayer transition metal dichalcogenides, *Phys. Rev. Lett.* **119**, 187402 (2017).
- [34] P.-F. Li and Z.-W. Wang, Optical absorption of Fröhlich polaron in monolayer transition metal dichalcogenides, *Journal of Applied Physics* **123**, 204308 (2018).
- [35] Q. Chen, W. Wang, and F. M. Peeters, Magneto-polarons in monolayer transition-metal dichalcogenides, *Journal of Applied Physics* **123**, 214303 (2018).
- [36] D. Van Tuan, B. Scharf, I. Žutić, and H. Dery, Intervalley plasmons in crystals, arXiv:1901.02567 (2019).
- [37] See Supplemental Material, which includes Refs. [38–49].
- [38] Thibault Sohler, Matteo Calandra, and Francesco Mauri, Two-dimensional Fröhlich interaction in transition-metal dichalcogenide monolayers: Theoretical modeling and first-principles calculations, *Phys. Rev. B* **94**, 085415 (2016).
- [39] M. Danovich, I. L. Aleiner, N. D. Drummond, and V. I. Fal’ko, Fast relaxation of photo-excited carriers in 2-d transition metal dichalcogenides, *IEEE Journal of Selected Topics in Quantum Electronics* **23**, 1–5 (2017).
- [40] M. A. Smondyrev, Diagrams in the polaron model, *Theoretical and Mathematical Physics* **68**, 653–664 (1986).
- [41] Yao Xiao, Zhi-Qing Li, and Zi-Wu Wang, Polaron effect on the bandgap modulation in monolayer transition metal dichalcogenides, *Journal of Physics: Condensed Matter* **29**, 485001 (2017).
- [42] R. P. Feynman, Slow electrons in a polar crystal, *Phys. Rev.* **97**, 660–665 (1955).
- [43] M. Matsuura, “Discontinuity of the surface polaron,” *Solid State Communications* **44**, 1471 – 1475 (1982).
- [44] W.J. Huybrechts, Ground-state energy and effective mass of a polaron in a two-dimensional surface layer, *Solid State Communications* **28**, 95 – 97 (1978).
- [45] Wu Xiaoguang, F. M. Peeters, and J. T. Devreese, Exact and approximate results for the ground-state energy of a Fröhlich polaron in two dimensions, *Phys. Rev. B* **31**, 3420–3426 (1985).
- [46] T Holstein, Studies of polaron motion: Part I. The molecular-crystal model, *Annals of Physics* **8**, 325 – 342 (1959).
- [47] Mingu Kang, Sung Won Jung, Woo Jong Shin, Yeongsup Sohn, Sae Hee Ryu, Timur K Kim, Moritz Hoesch, and Keun Su Kim, Holstein polaron in a valley-degenerate two-dimensional semiconductor, *Nat. Mater.* **17**, 676 (2018).
- [48] J. Ribeiro-Soares, R. M. Almeida, E. B. Barros, P. T. Araujo, M. S. Dresselhaus, L. G. Cançado, and A. Jorio, Group theory analysis of phonons in two-dimensional transition metal dichalcogenides, *Phys. Rev. B* **90**, 115438 (2014).
- [49] Bruno R. Carvalho, Yuanxi Wang, Sandro Mignuzzi, Debdulal Roy, Mauricio Terrones, Cristiano Fantini, Vincent H. Crespi, Leandro M. Malard, and Marcos A. Pimenta, Intervalley scattering by acoustic phonons in two-dimensional MoS₂ revealed by double-resonance Raman spectroscopy, *Nat. Commun.* **8**, 14670 (2017).
- [50] We neglect the difference of the electron effective masses in the two spin subbands due to spin-orbit coupling and $\mathbf{k} \cdot \mathbf{p}$ mixing.
- [51] For the sake of simplicity, the overall shift of the conduction band $\propto \beta_{\mathbf{K}} \ln(E_Q/\Delta_{cb})$ is disregarded.
- [52] I. B. Levinson and É. I. Rashba, Bound states of electrons and excitons with optical phonons in semiconductors, *Soviet Physics Uspekhi* **15**, 663 (1973).
- [53] V. L. Gurevich and Y. A. Firsov, A new oscillation mode of the longitudinal magnetoresistance of semiconductors, *JETP* **20**, 489 (1965).
- [54] Y. A. Firsov, V. L. Gurevich, R. V. Parfeniev, and S. S. Shalyt, Investigation of a new type of oscillations in the magnetoresistance, *Phys. Rev. Lett.* **12**, 660 (1964).
- [55] A. Molina-Sánchez and L. Wirtz, Phonons in single-layer and few-layer MoS₂ and WS₂, *Phys. Rev. B* **84**, 155413 (2011).
- [56] K. Kaasbjerg, K. S. Thygesen, and K. W. Jacobsen, Phonon-limited mobility in *n*-type single-layer MoS₂ from first principles, *Phys. Rev. B* **85**, 115317 (2012).
- [57] Z. Jin, X. Li, J. T. Mullen, and K. W. Kim, Intrinsic transport properties of electrons and holes in monolayer transition-metal dichalcogenides, *Phys. Rev. B* **90**, 045422 (2014).
- [58] Lifa Zhang and Qian Niu, Chiral phonons at high-symmetry points in monolayer hexagonal lattices, *Phys. Rev. Lett.* **115**, 115502 (2015).
- [59] Hanyu Zhu, Jun Yi, Ming-Yang Li, Jun Xiao, Lifa Zhang, Chih-Wen Yang, Robert A. Kaindl, Lain-Jong Li, Yuan Wang, and Xiang Zhang, Observation of chiral phonons, *Science* **359**, 579–582 (2018).
- [60] J. P. Echeverry, B. Urbaszek, T. Amand, X. Marie, and I. C. Gerber, Splitting between bright and dark excitons in transition metal dichalcogenide monolayers, *Phys. Rev. B* **93**, 121107(R) (2019).
- [61] The carrier densities in the transport measurements for holes are similar to the measurements for electrons discussed above.

- [62] C. Chen, J. Avila, S. Wang, Y. Wang, M. Mucha-Kruczyński, C. Shen, R. Yang, B. Nosarzewski, T. P. Devereaux, G. Zhang, *et al.*, Emergence of interfacial polarons from electron–phonon coupling in graphene/h-BN van der waals heterostructures, *Nano Lett.* **18**, 1082 (2018).
- [63] M. Goryca, J. Li, A. V. Stier, S. A. Crooker, T. Taniguchi, K. Watanabe, E. Courtade, S. Shree, C. Robert, B. Urbaszek, and X. Marie, Revealing exciton masses and dielectric properties of monolayer semiconductors with high magnetic fields, arXiv e-prints 1904.03238 (2019)

Supplemental Information for Intervalley Polaron in Atomically Thin Transition Metal Dichalcogenides

M.M. Glazov, M.A. Semina
Ioffe Institute, 194021 St. Petersburg, Russia

C. Robert, B. Urbaszek, T. Amand, X. Marie
Université de Toulouse, INSA-CNRS-UPS, LPCNO, 135 Av. Rangueil, 31077 Toulouse, France

CONTENTS

SI. Intravalley polaron	1
A. Perturbative derivation	1
B. Feynman variational approach	2
SII. Intervalley polaron	2
A. Renormalization of Landau levels	2
B. Relation to Holstein polaron	3
SIII. Symmetry of the involved phonon modes	3
References	4

SI. INTRAVALLEY POLARON

In this section we study electron-optical phonon polaron in TMD monolayers. Here we consider only transitions with the intermediate states in the same valley. This introductory part is needed in order to introduce definitions and to justify the first-order calculation of the intervalley polaron effect.

In TMD monolayers the intravalley electron-phonon interaction can be provided by two mechanisms. First, there is the Fröhlich interaction between the electron and dielectric polarization induced by the optical phonons in the monolayer [S1–S3] which in two-dimensional materials has a non-divergent form with the scattering matrix element

$$M_{\mathbf{q}}^{(F)} = \frac{C_F}{1 + 2\pi\alpha q}, \quad (\text{S1})$$

where \mathbf{q} is the phonon wavevector, C_F is bare Fröhlich interaction constant, and α is the polarizability of the layer [S2, S3]. Also, the deformation potential interaction is possible with [S1, S4]

$$M_{\mathbf{q}}^{(DP)} = D_{opt}. \quad (\text{S2})$$

In this model the optical phonon deformation potential is taken to be independent of \mathbf{q} (for wavevectors smaller than the Brillouin zone size). In both cases, the matrix element is regular at $\mathbf{q} \rightarrow 0$ and in many situations one can consider the coupling as q -independent.

A. Perturbative derivation

Here we derive the polaron shift and the correction to the effective mass of the electron for the intravalley, Fröhlich-like, polaron in TMD ML. We consider dispersionless optical phonon with the frequency Ω_0 and disregard the wavevector dependence of the matrix element replacing $M_{\mathbf{q}}$ by the constant M_0 .

It is convenient to measure energies in the units of optical phonon energy, $\hbar\Omega_0$, and present the electron momentum in the dimensionless form

$$\mathbf{w} = \frac{\mathbf{p}}{\sqrt{2m\hbar\Omega_0}}.$$

We follow the method of Ref. [S5] in order to analyze the polaron corrections in the second and fourth order perturbation theory. In the dimensionless units the second-order (with respect to $M_{\mathbf{q}}$) self-energy reads

$$\Sigma_1 = -\frac{\beta}{(2\pi)^2} \int \frac{d\mathbf{k}}{1 - 2\mathbf{w} \cdot \mathbf{k} + k^2}. \quad (\text{S3})$$

Here

$$\beta = 2m\hbar\Omega_0 \mathcal{S} |M_0/\hbar\Omega_0|^2 / \hbar^2, \quad (\text{S4})$$

is the dimensionless coupling constant, \mathbf{k} is the dimensionless phonon momentum. Integral in Eq. (S3) formally diverges (this is due to the fact that we neglect the momentum dependence of the electron-phonon matrix element). The electron energy renormalization in the first order in β reads

$$\mathcal{E}_1 = -\frac{\beta}{4\pi} (2 \ln Q + w^2), \quad (\text{S5})$$

where Q is the cut-off wavevector. The correction to the effective mass is finite and the renormalized mass reads

$$m_1^* = m \left(1 + \frac{\beta}{4\pi} \right) = m \left(1 + \frac{m\mathcal{S}|M_0|^2}{2\pi\hbar^3\Omega_0} \right). \quad (\text{S6})$$

This result is in agreement with Eq. (6) of the main text at $\Delta_{cb} = 0$.

Equation (S5) can be applied also to a valence band with corresponding parameters, see Ref. [S6] where the effect for intravalley Fröhlich polaron was discussed. The intravalley polaron corrections to the dispersion of the conduction and valence have the same order of magnitude [S7].

For Fröhlich polaron in three dimensions the higher order corrections in the coupling constant are small in

the weak coupling regime. We demonstrate that this is also the case for the TMD MLs. In the fourth-order in electron-phonon interaction we have three contributions

$$\Sigma_2^{(1)} = -\frac{\beta^2}{(2\pi)^4} \int \frac{dkdq}{(1-2\mathbf{w}\cdot\mathbf{k}+k^2)^2(2-2\mathbf{w}\cdot\mathbf{q}+q^2)}, \quad (\text{S7})$$

$$\Sigma_2^{(2)} = -\frac{\beta^2}{(2\pi)^4} \int \frac{dkdq}{(1-2\mathbf{w}\cdot\mathbf{k}+k^2)[2-2\mathbf{w}\cdot(\mathbf{k}+\mathbf{q})+(\mathbf{k}+\mathbf{q})^2](1-2\mathbf{w}\cdot\mathbf{q}+q^2)}, \quad (\text{S8})$$

$$\Sigma_2^{(3)} = \frac{\beta^2}{(2\pi)^4} \int \frac{dkdq}{(1-2\mathbf{w}\cdot\mathbf{k}+k^2)^2(1-2\mathbf{w}\cdot\mathbf{q}+q^2)}, \quad (\text{S9})$$

stemming from “ladder”, “crossing” and “disconnected” diagrams. Although each of $\Sigma_2^{(1)}$ and $\Sigma_2^{(3)}$ diverge logarithmically, their sum is finite

$$\mathcal{E}_2^{(1+3)} = \frac{\beta^2 \ln 2}{16\pi^2} + \frac{\beta^2(\ln 2 + 1/2)}{16\pi^2} w^2, \quad (\text{S10})$$

The self-energy $\Sigma_2^{(2)}$ can be integrated numerically only (after analytical integration over the angles of \mathbf{k} and \mathbf{q} we arrive at the bulky expression which needs to be numerically integrated over the absolute values of the wavevectors):

$$\mathcal{E}_2^{(2)} \approx -\frac{\beta^2}{16\pi^4} (18.08 + 13.98w^2), \quad (\text{S11})$$

As a result, up to the second order we have

$$\mathcal{E}_{1,2} = -\frac{\beta}{4\pi} (2\ln Q + w^2) - \beta^2 (0.0072 + 0.0014w^2). \quad (\text{S12})$$

The mass enhancement is finally given by

$$m^* = m \left(1 + \frac{\beta}{4\pi} + 0.0077\beta^2 \right). \quad (\text{S13})$$

B. Feynman variational approach

Following Refs. [S8–S11] we obtain the following expression for the variational functional (derived in the path-integral approach)

$$E\{V, W\} = \frac{(V-W)^2}{2V} - \beta \int_0^\infty du e^{-u} \mathcal{I}(u; V, W), \quad (\text{S14})$$

$$\mathcal{I}(u; V, W) = \frac{1}{2(2\pi)^2} \int d\mathbf{k} \exp[-F(u; V, W)k^2],$$

$$F(u; V, W) = \frac{W^2}{2V^2} u + \frac{V^2 - W^2}{2V^3} (1 - e^{-uV}).$$

where V and W are the variational parameters whose minimization (V^*, W^*) yields the polaron shift. Equations above are valid for the polaron at rest. The renormalization of the effective mass can be readily calculated as

$$\frac{m^*}{m} = 1 + \beta \int_0^\infty du e^{-u} \mathcal{I}'(u; V^*, W^*) \quad (\text{S15})$$

$$\mathcal{I}'(u; V^*, W^*) = \frac{1}{2(2\pi)^2} \int d\mathbf{k} \exp[-F(u; V^*, W^*)k^2] \frac{k^2 u^2}{2}.$$

In the linear in β regime one can put $V^* = W^*$, thus $F = u/2$ and Eqs. (S14), (S15) pass to Eq. (S5) and (S6). In the second order in α we obtain (minimization yields $V^* = (1 + \epsilon)W^*$, $\epsilon \ll 1$, $W^* \approx 7.577$)

$$\mathcal{E} = -\frac{\beta \ln Q}{2\pi} - 0.0034\beta^2, \quad \frac{m^*}{m} = 1 + \frac{\beta}{4\pi} + 0.0069\beta^2. \quad (\text{S16})$$

The analysis above demonstrates that the fourth-order (with respect to $M_{\mathbf{q}}$) corrections are indeed small. Therefore, in the remaining parts we will consider the second-order (with respect to $M_{\mathbf{q}}$, i.e., linear in β) corrections only.

III. INTERVALLEY POLARON

A. Renormalization of Landau levels

The correction to the energy of electron on n -th Landau level is given, in the second-order in the intervalley electron-phonon interaction ($\propto |M_{\mathbf{K}}|^2$ or $\propto \beta_{\mathbf{K}}$), by

$$\delta E_{n,\pm} = \sum_{\mathbf{q}, n'k'_y} \frac{|M_{\mathbf{K}}|^2 |\langle n'k'_y | e^{i\mathbf{q}\cdot\mathbf{r}} | nk_y \rangle|^2}{\hbar\omega_c(n-n') - \hbar\Omega_{\mathbf{K}} \pm \Delta_{cb}}, \quad (\text{S17})$$

where $\omega_c = |eB_z/mc|$ is the cyclotron frequency, $|nk_y\rangle$ is the Landau level wavefunction, and \mathbf{q} is the phonon wavevector (minus \mathbf{K} , the intervalley wavevector). We

use the Landau gauge with the vector potential $\mathbf{A} = [0, B_z x, 0]$; z is the monolayer normal, x and y are the axes in the sample plane. As discussed in the main text, we neglect the phonon dispersion and the dependence of the electron-phonon interaction matrix element on the phonon wavevector. The matrix element of the transition between the Landau levels can be expressed as [S12]

$$\langle n' k'_y | e^{i\mathbf{q}\mathbf{r}} | n k_y \rangle = \delta_{k'_y, k_y + q_y} Q_n^{n'-n}(u), \quad (\text{S18})$$

where $u = q^2 l_B^2 / 2$ and $l_B = \sqrt{\hbar c / |e B_z|}$ is the magnetic length,

$$Q_n^{n'-n}(u) = \frac{e^{-u/2} u^{(n'-n)/2}}{\sqrt{n'! n!}} L_n^{(n'-n)}(u),$$

$$\delta E_{n,\pm} - \delta E_{n-1,\pm} = -\frac{\beta_{\mathbf{K}} \hbar \omega_c}{4\pi} \frac{\hbar \Omega_{\mathbf{K}} + \Delta_{cb}}{\hbar \Omega_{\mathbf{K}} \mp \Delta_{cb}} \sum_{n'=0}^{\infty} \left[\frac{1}{1 + \eta_{\pm}(n' - n)} - \frac{1}{1 + \eta_{\pm}(n' - n + 1)} \right] = -\frac{\beta_{\mathbf{K}} \hbar \omega_c}{4\pi} \frac{\hbar \Omega_{\mathbf{K}} + \Delta_{cb}}{\hbar \Omega_{\mathbf{K}} \mp \Delta_{cb}} \frac{1}{1 - \eta_{\pm} n}, \quad (\text{S20})$$

where $\eta_{\pm} = \hbar \omega_c / (\mp \Delta_{cb} + \hbar \Omega_{\mathbf{K}})$. Note that in order to calculate the sum one has to make a replacement $n' \rightarrow n + 1$ in the second term. Equation (S20) is in agreement with Eq. (9) of the main text.

B. Relation to Holstein polaron

It is instructive to discuss the difference between our model and the Holstein polaron [S13, S14] where the polaron radius is on the order of lattice constant. Indeed some measurements of strong band gap renormalization in surface doped thick layers of MoS₂ were interpreted recently on the basis of Holstein polaron [S15]. Although in our case, the involved wavevectors of phonons correspond to the BZ size and the phonon wavelengths are on the order of the lattice constant, the direct analogy with the Holstein polaron is not so relevant: In the Holstein polaron approach the polaron energy E_{pol} roughly corresponds to the band width. In contrast, in our case the weak coupling regime is realized: $\beta_{\mathbf{K}} \lesssim 1$ thus, the polaron energy $E_{pol} \sim \beta_{\mathbf{K}} \hbar \Omega_{\mathbf{K}}$ is negligible compared with the band width. The calculation of intervalley Holstein polaron characteristics in ML TMDs is beyond the scope of this paper.

and

$$L_n^m(u) = e^u u^{-m} \frac{d^n}{du^n} (e^u u^{n+m}),$$

is the generalized Laguerre polynomial. Here we assumed $n' > n$, similar expressions can be written for $n' \leq n$.

The summation over k'_y is removed by using the y -component of momentum conservation δ -function and the summation over \mathbf{q} can be performed by virtue of

$$\int_0^{\infty} du \left| Q_n^{n'-n}(u) \right|^2 = 1,$$

yielding

$$\delta E_{n,\pm} = \frac{S |M_{\mathbf{K}}|^2}{2\pi l_B^2} \sum_{n'=0}^{\infty} \frac{1}{\hbar \omega_c (n - n') - \hbar \Omega_{\mathbf{K}} \pm \Delta_{cb}}. \quad (\text{S19})$$

As above, this sum is divergent logarithmically, but we are interested only in the renormalization of Landau level distances. Thus, the correction to $\hbar \omega_c$ for the transition between n -th and $n - 1$ -th Landau levels reads

III. SYMMETRY OF THE INVOLVED PHONON MODES

Table I. Irreducible representations of the C_{3h} point group and characters of the relevant elements, $\omega = \exp(2\pi i/3)$. The center of the point group transformations corresponds to the center of hexagon.

		e	C_3	S_3	σ_h	Basic functions
A'	K_1	1	1	1	1	$x^2 + y^2; z^2$
E'_1	K_2	1	ω	ω	1	$x + iy; (x - iy)^2$
E'_2	K_3	1	ω^2	ω^2	1	$x - iy; (x + iy)^2$
A''	K_4	1	1	-1	-1	z
E''_1	K_5	1	ω	$-\omega$	-1	$S_x + iS_y; (S_x - iS_y)^2$
E''_2	K_6	1	ω^2	$-\omega^2$	-1	$S_x - iS_y; (S_x + iS_y)^2$

We consider phonons which provide the electron mixing between the \mathbf{K} and \mathbf{K}' points of the BZ. Note that in the \mathbf{K} valley the interband optical transition is allowed in σ^+ polarization and in the \mathbf{K}' valley is in the σ^- polarization. The wavevector of such phonon equals to \mathbf{K} , see inset in Fig. 1 of the main text. Note that for simplicity we consider the phonon absorption process and the transfer $\mathbf{K} \rightarrow \mathbf{K}'$, the analysis of the emission process is similar, but requires to consider the phonons

in the \mathbf{K}' point of the BZ. In order to determine the selection rules it is needed to consider the corresponding wavevector group C_{3h} . Since we neglect the spin mixing, it is sufficient to consider only transformation of the orbital parts of the Bloch functions of electrons. Thus, disregarding the spin and spin-orbit coupling the basic functions of the conduction band top transform according to $\mathcal{D}_{\mathbf{K}} = K_2 (E'_1)$ in the \mathbf{K} valley and according to $\mathcal{D}_{\mathbf{K}'} = K_3 (E'_2)$ in the \mathbf{K}' valley.

It follows from Ref. [S16] that the phonons at the \mathbf{K} point of the BZ transform according to the following irreducible representations of the C_{3h} point group ($2Hc$ -

polytype, $N = 1$):

$$2K_1, K_2, 2K_3, K_4, 2K_5, K_6. \quad (\text{S21})$$

There are 9 phonon modes in total (3 atoms in the unit cell). Note that in the \mathbf{K}' point the phonon modes are complex conjugate, $2K_1, 2K_2, K_3, K_4, K_5, 2K_6$. In order to enable the electron mixing, the symmetry of the phonon mode \mathcal{D}_{ph} should be such that the direct product of the representations

$$\mathcal{D}_{\mathbf{K}'}^* \otimes \mathcal{D}_{ph} \otimes \mathcal{D}_{\mathbf{K}} = K_3 \otimes \mathcal{D}_{ph}, \quad (\text{S22})$$

contains the identical one, K_1 (or A'). This is possible only for the phonon of K_2 symmetry. Thus, only one phonon mode is allowed for such a transfer [S1, S17–S20].

-
- [S1] Kristen Kaasbjerg, Kristian S. Thygesen, and Karsten W. Jacobsen, “Phonon-limited mobility in n -type single-layer MoS₂ from first principles,” *Phys. Rev. B* **85**, 115317 (2012).
- [S2] Thibault Sohier, Matteo Calandra, and Francesco Mauri, “Two-dimensional Fröhlich interaction in transition-metal dichalcogenide monolayers: Theoretical modeling and first-principles calculations,” *Phys. Rev. B* **94**, 085415 (2016).
- [S3] M. Danovich, I. L. Aleiner, N. D. Drummond, and V. I. Fal’ko, “Fast relaxation of photo-excited carriers in 2-d transition metal dichalcogenides,” *IEEE Journal of Selected Topics in Quantum Electronics* **23**, 1–5 (2017).
- [S4] Zhenghe Jin, Xiaodong Li, Jeffrey T. Mullen, and Ki Wook Kim, “Intrinsic transport properties of electrons and holes in monolayer transition-metal dichalcogenides,” *Phys. Rev. B* **90**, 045422 (2014).
- [S5] M. A. Smondyrev, “Diagrams in the polaron model,” *Theoretical and Mathematical Physics* **68**, 653–664 (1986).
- [S6] Yao Xiao, Zhi-Qing Li, and Zi-Wu Wang, “Polaron effect on the bandgap modulation in monolayer transition metal dichalcogenides,” *Journal of Physics: Condensed Matter* **29**, 485001 (2017).
- [S7] Dinh Van Tuan, Benedikt Scharf, Igor Žutić, and Hanan Dery, “Intervalley plasmons in crystals,” arXiv:1901.02567 (2019).
- [S8] R. P. Feynman, “Slow electrons in a polar crystal,” *Phys. Rev.* **97**, 660–665 (1955).
- [S9] M. Matsuura, “Discontinuity of the surface polaron,” *Solid State Communications* **44**, 1471 – 1475 (1982).
- [S10] W.J. Huybrechts, “Ground-state energy and effective mass of a polaron in a two-dimensional surface layer,” *Solid State Communications* **28**, 95 – 97 (1978).
- [S11] Wu Xiaoguang, F. M. Peeters, and J. T. Devreese, “Exact and approximate results for the ground-state energy of a Fröhlich polaron in two dimensions,” *Phys. Rev. B* **31**, 3420–3426 (1985).
- [S12] V. L. Gurevich and Yu. A. Firsov, “A new oscillation mode of the longitudinal magnetoresistance of semiconductors,” *JETP* **20**, 489 (1965).
- [S13] T Holstein, “Studies of polaron motion: Part I. The molecular-crystal model,” *Annals of Physics* **8**, 325 – 342 (1959).
- [S14] Alexandre S. Alexandrov and Jozef T. Devreese, *Advances in Polaron Physics* (Springer Berlin Heidelberg, 2010).
- [S15] Mingu Kang, Sung Won Jung, Woo Jong Shin, Yeongsup Sohn, Sae Hee Ryu, Timur K Kim, Moritz Hoesch, and Keun Su Kim, “Holstein polaron in a valley-degenerate two-dimensional semiconductor,” *Nat. Mater.* **17**, 676 (2018).
- [S16] J. Ribeiro-Soares, R. M. Almeida, E. B. Barros, P. T. Araujo, M. S. Dresselhaus, L. G. Cançado, and A. Jorio, “Group theory analysis of phonons in two-dimensional transition metal dichalcogenides,” *Phys. Rev. B* **90**, 115438 (2014).
- [S17] Yang Song and Hanan Dery, “Transport theory of monolayer transition-metal dichalcogenides through symmetry,” *Phys. Rev. Lett.* **111**, 026601 (2013).
- [S18] Bruno R. Carvalho, Yuanxi Wang, Sandro Mignuzzi, Debdulal Roy, Mauricio Terrones, Cristiano Fantini, Vincent H. Crespi, Leandro M. Malard, and Marcos A. Pimenta, “Intervalley scattering by acoustic phonons in two-dimensional MoS₂ revealed by double-resonance Raman spectroscopy,” *Nat. Commun.* **8**, 14670 (2017).
- [S19] Lifa Zhang and Qian Niu, “Chiral phonons at high-symmetry points in monolayer hexagonal lattices,” *Phys. Rev. Lett.* **115**, 115502 (2015).
- [S20] Hanyu Zhu, Jun Yi, Ming-Yang Li, Jun Xiao, Lifa Zhang, Chih-Wen Yang, Robert A. Kaindl, Lain-Jong Li, Yuan Wang, and Xiang Zhang, “Observation of chiral phonons,” *Science* **359**, 579–582 (2018).